Available online at www.sciencedirect.com

ScienceDirect

Procedia Structural Integrity 34 (2021) 121–128

Structural Integrity Procedia

www.elsevier.com/locate/procedia

The second European Conference on the Structural Integrity of Additively Manufactured Materials

Experimental and numerical analysis of fatigue cracks emanating from internal defects in Ti6Al4V SLM

Santiago Aguado-Montero*, Carlos Navarro, Jesús Vázquez, Jaime Domínguez

Departamento de Ingeniería Mecánica y Fabricación
Escuela Técnica Superior de Ingeniería. Universidad de Sevilla
Camino de los descubrimientos s/n, 41092 Sevilla-España
** Contact: saguado@us.es*

Abstract

In the present work a series of fatigue tests on Ti6Al4V SLM parts are analyzed via both SEM and confocal microscopy. On the one hand, fracture surfaces are studied, and a common pattern is found, formed by a series of different textures which show the complex crack front evolution from crack initiation in a particular internal defect to complete failure. On the other hand, fatigue strength is observed to highly depend on the defect where initiation takes place, so experimental observation of that critical entity is carried out. Both defect location within the specimen and shape are studied, considering the crack-like or blunt feature of every defect. Once experimental analysis is complete, numerical simulation is attempted. By making use of critical defect and residual stress measurements obtained experimentally, both fatigue strength and crack front evolution are estimated.

Keywords: Fatigue, SLM, Titanium alloy, Critical defect SEM and confocal microscopy, Crack growth simulation.

1. Introduction

Fatigue loading is a very common issue that engineers face when dealing with additive manufactured metallic parts. However, the fact is that not only components have a significantly worse fatigue resistance, but also their fatigue lives are difficult to predict. There exists a large variability from one specimen to another due to a remarkable difference in variables such as porosity size and distribution.

Porosity is a random result of two different phenomena, as discussed in [1]. The first one is gas entrapment in the matrix. These gases could either be part of the inert atmosphere surrounding the manufacturing process or belong to the matrix itself, due to metallic powder evaporation. Both situations produce a blunt, mostly spherical void. The second one is small laser fluctuations that lead to local inter-layer debonding, i.e., freshly melted powder does not

10.1016/j.prostr.2021.12.018

attach in a certain region to the previous layer. As a result, a very sharp, crack-like defect is left in the matrix. Both situations described here take place in random positions in the matrix, so defect location, size or shape are not known in advance.

According to Yates et al [2], since porosity is a random output from the manufacturing process, conventional fatigue analysis such as S-N or ε-N curves do not provide enough information to assess fatigue life in a certain component. Because of the porosity being different from specimen to specimen, a huge variability in results is obtained when using these simple techniques. To solve this problem, Yates proposes a probabilistic approach, i.e., including porosity statistics into the analysis. This fatigue life dependence on porosity is also reported by other authors [3-5].

The aim of the current work is to stablish some method to generalize the probabilistic approach. We focus on building a model to simulate the evolution of a crack emanating from a given defect until final failure. A set of experiments is analyzed: fatigue lives, fracture surfaces, critical defects geometry and residual stresses are considered. After this stage is complete, the equations governing crack evolution in the simulation are discussed. An initiation-propagation fatigue model [6] is used and its results are compared with experiments.

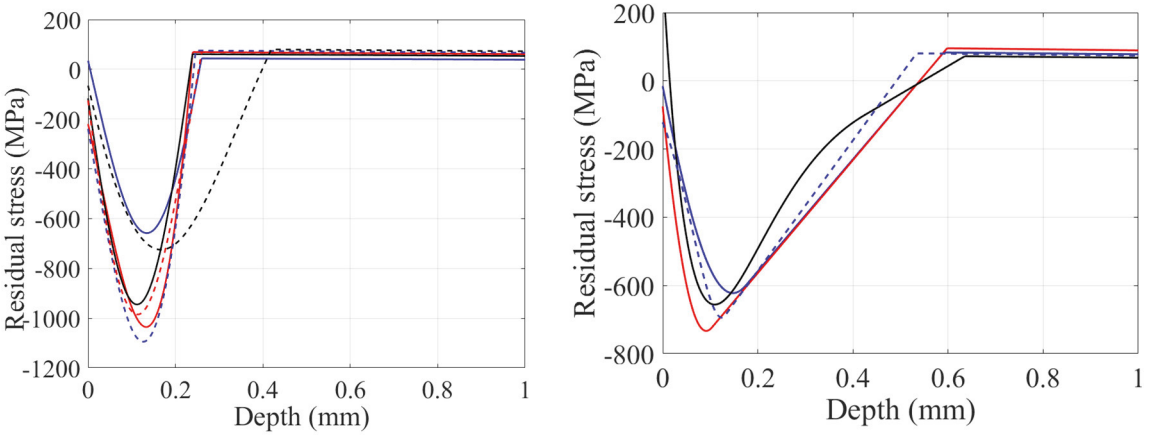

Fig. 1. Measured residual stresses in (left) shot peening and (right) laser peening.

2. Experiments

The material tested is the alloy Ti6Al4V manufactured via Selective Laser Melting (SLM). Tests were conducted on specimens with a cross section of 22x10 mm in a four-point bending setup, with load ratio R=0.1. In addition to this external load, a subset of the specimens received surface treatment consisting of either laser or shot peening, resulting in substantial compressive residual stresses close to the treated surface. Before these surface treatments, all specimens were sand blasted and heat treated to ensure that no residual stresses due to the manufacturing process were present. Figure 1 shows residual stress measurements [7]. Provided the load ratio was kept as R=0.1, only half of the specimen's bending section was subjected to tensile stress so only half of its surface received surface treatment, since the rest of the section was not susceptible to crack initiation.

In the present paper we are interested in cracks emanating from internal defects. The presence of compressive residual stresses in regions close to the surface inhibits superficial crack initiation, turning embedded crack formation into a more probable event. For this reason, only those specimens with surface treatment whose cracks started from internal defects are analyzed.

Note that positive load ratios keep the applied stresses in the surface treated region strictly positive, so that residual stresses do not disappear via reversed plastic deformation. On the contrary, they remain active for a significant fraction of the specimen fatigue life.

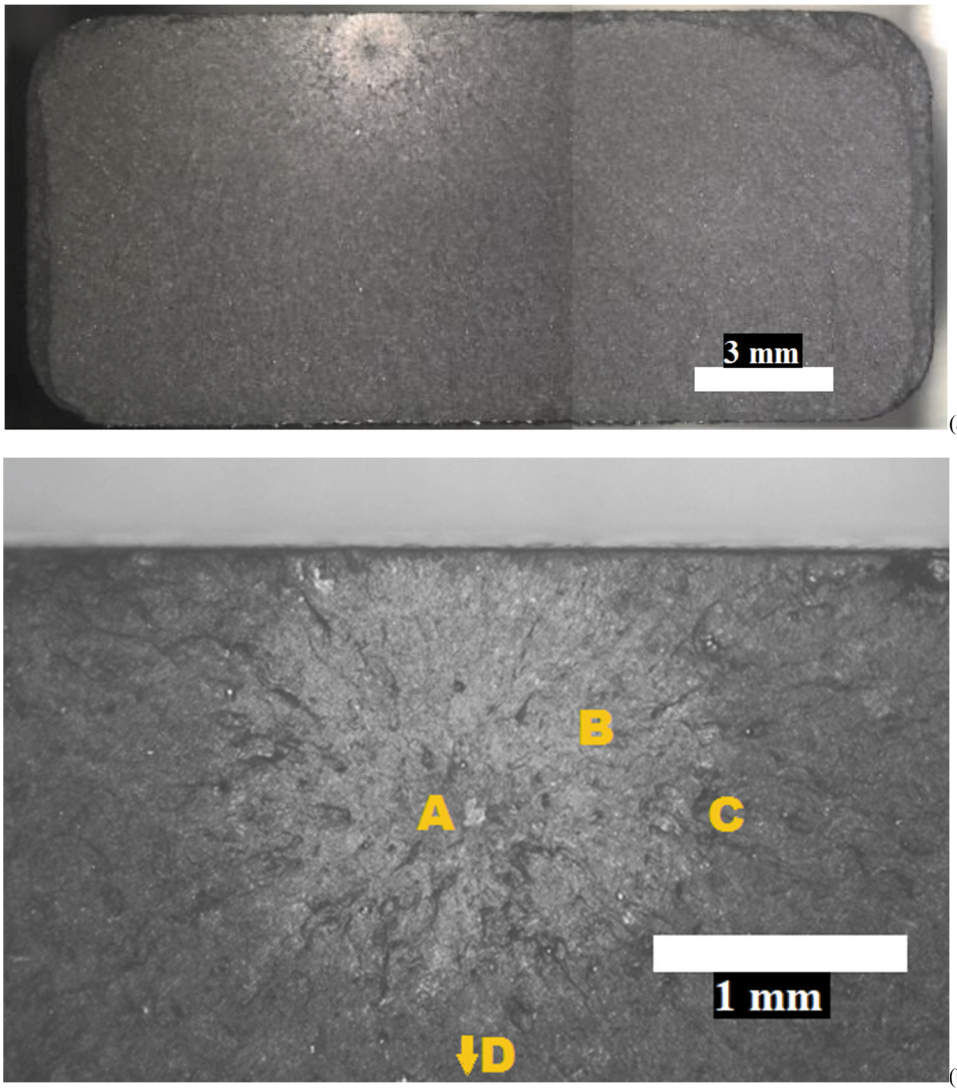

Fig. 2. (a) Fracture surface photograph in the cross section (22 x 10 mm) of a laser peened specimen, (b) detail of defect area [7].

3. Experimental results

3.1.- Fracture surfaces

Those specimens which suffered from internal crack initiation show a very peculiar evolution in their fracture surface textures. FEI Teneo SEM and Sensofar S neox confocal microscopes were used to analyze these surfaces. Four different regions can be observed, as can be followed from Figures 2 and 3.

A very microstructurally textured region takes place close to the internal defect. This region covers a distance of a few hundred microns (Figure 3a) and follows closely the typical acicular microstructure of a Ti alloy. According to Zhai et al [8], this is a result of cracks growing just above the fatigue crack growth threshold, which is exactly the case according to the simulations discussed later.

Surrounding the microstructurally textured region, a very bright, elliptical zone, almost tangent to the free surface can be easily seen, especially with the naked eye (Figure 2). When observed with SEM, a significantly irregular texture is observed (Figure 3b), with no microstructural characteristics nor striations visible. It is hypothesized (the consequences of this will be discussed later) this zone to be the embedded crack growth region, i.e., the shape the

crack had just before it reached the free surface and transitioned into a superficial semielliptical crack. Note that this elliptical region is not necessarily centered in the initial defect.

As one moves farther from the defect, more and more striations are visible (Figure 3c). At the SEM level, a sharp transition from irregular texture to striations was not observed, but rather a smooth increase in the appearance of striations. Finally, once the stress intensity factor reaches a high enough value, a plastically deformed, dimpled surface is obtained (Figure 3d).

3.2.- Critical defects

Critical defects geometry and location in the specimen are important variables in fatigue life assessment of internal initiated cracks. Three main information points need to be collected for every specimen:

Defect projected size. Figure 4 shows two fracture surfaces where the initial critical defect is clearly seen. To associate a numerical value to these complex-shaped defects, an equivalent ellipse with the same area as the real defect and the same aspect ratio has been defined. The aspect ratio is defined as the ratio of maximum defect length in both directions perpendicular to the rectangular section sides.

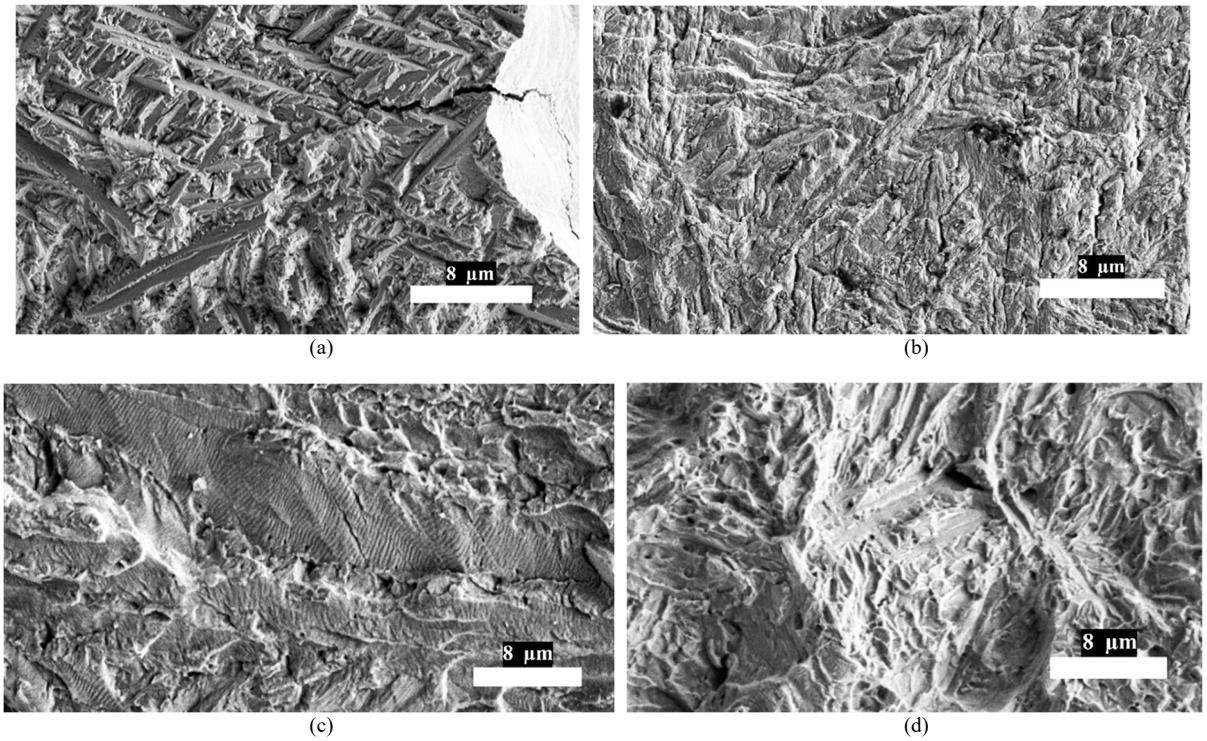

Fig. 3. Fracture surface evolution. (a) Microstructurally textured fracture surface, (b) irregular bright region, (c) striated zone, (d) dimpled fracture surface.

Defect distance to free surface. If one tries to imagine the evolution of a crack emanating from an internal defect, considering it will grow perpendicular to the first principal stress according to Fatemi et al [9], the crack will increase its size and modify its shape since stresses are not the same along different crack front points. If it is presumed that the initial defect is out of the residual stressed region, the tensile loads will always be higher in the crack point closer to the free surface, due to the bending setup. If this is the case, the crack will propagate mainly towards the closest free surface.

Eventually, it will reach this surface and turn into a superficial crack. With all this said, defect distance to free surface is a critical variable, since not only stresses will be higher the closer the defect is to free surface, but also cracks will need a shorter evolution to reach this free surface. According to simulations discussed later in this paper, embedded

crack evolution is usually more than 90% of total fatigue life.

Defect type. As we mentioned in the introductory section, two different kinds of defects are formed in SLM specimens, namely blunt and crack-like defects, depending on the process by which they were formed. Since it is not known in advance which of the defects are crack-like and which of them are not, confocal microscopy was carried out to collect data about defect depth. Figure 4 shows two different examples of crack-like and blunt defects.

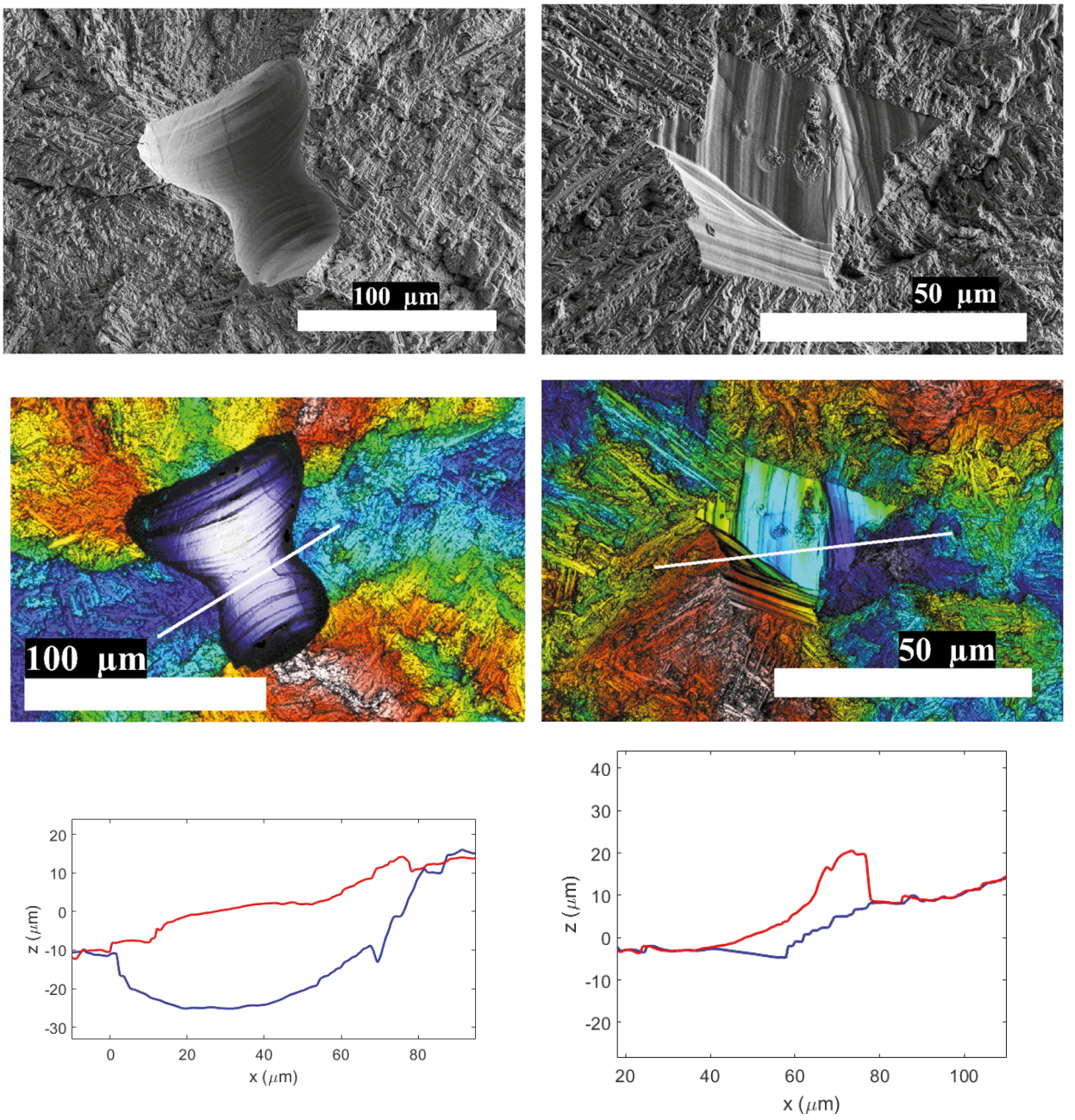

Fig. 4. SEM, confocal microscopy, and cross sections of both upper and lower sides of fractured defects (Z axis is parallel to the loading direction) of two different types of defects. All three pictures on the left column represent a blunt defect while those on the right column represent a crack like defect.

4. Simulation model

In the present work, crack initiation life was estimated via the model proposed in [6]. However, preliminary calculations suggested that the stress field around critical defects was high enough to ignore the amount of cycles to initiate a crack, thus considering crack propagation as the only contribution to fatigue life.

Crack propagation of an elliptical embedded or semielliptical surface crack has been modelled with the following crack propagation law:

$$\frac{da_i}{dN} = C\left(\Delta K_i^n - \left(\Delta K_{th}\left(\frac{a_i^f}{a_i^f + a_0^f + l_0^f}\right)^{\frac{1}{2f}}\right)^n\right) \tag{1}$$

where the last term in the equation accounts for short crack behavior, as proposed by Navarro et al [6]. To solve this differential equation system, the main variable to be calculated is the stress intensity factor. Since residual stresses need to be taken into consideration, the weight function technique is used. Both embedded and superficial weighting functions were obtained from the literature [10]. This reference provides the required data as a function of standard tensile and bending stress intensity factor results, which were obtained from [11]. However, these standard solutions do not provide valuable information when the remaining ligament tends to zero, so a correction factor was incorporated to the embedded solution via comparison with NASGRO® software solutions. This correction factor is very important due to its impact over embedded to superficial crack transition, which takes place once the stress intensity factor in the closest point to free surface reaches the material's fracture toughness.

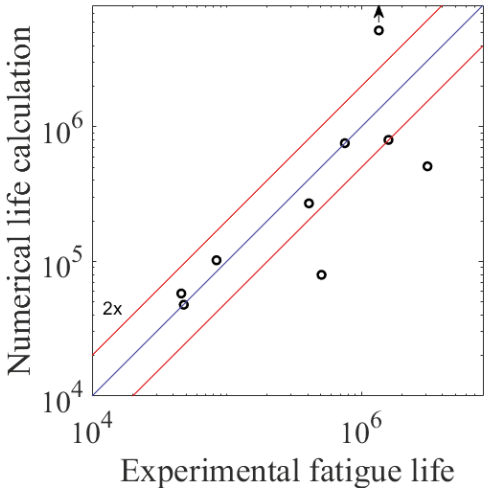

Fig. 5. Experimental and numerical fatigue life results.

5. Simulation results

The application of the fatigue life assessment model described in the previous sections yields the results shown in Figure 5. As can be observed, only three predicted results were not within a factor of two scatter band. One of the specimens that lay out of this band failed because of very close to threshold crack growth. Indeed, a slight variation in the fatigue growth threshold (±0.5 MPa√m) suffices to obtain more precise predictions. The other failed predictions might be due to a very nonelliptical defect shape, leading to a misrepresentation of the defect if the square root of area method is employed. Additional inaccuracies can be expected due to errors in residual stress measurements.

Crack propagation simulations show that initial aspect ratios in the defects were not important variables. On the contrary, cracks' aspect ratios rapidly evolved and stabilized in different values, depending on residual stresses acting near the free surface. As mentioned before, cracks tend to grow mainly towards free surface and, as the remaining

ligament tends to zero, the stress intensity factor experiments an intense increasement, thanks to the correction factor included in the stress intensity factor calculations, resulting in embedded to superficial crack transition.

Another important aspect related to the embedded to superficial crack transition is the very close correlation obtained between experimental fracture surface bright region (Figure 2) and embedded crack shape just before transition took place, as shown in Figure 6. This confirms cracks are evolving with an elliptical shape until the very moment in which embedded to superficial crack transition takes place. Moreover, the embedded cracks reach a state where the remaining ligament is almost inexistent, once again matching fracture surfaces observed.

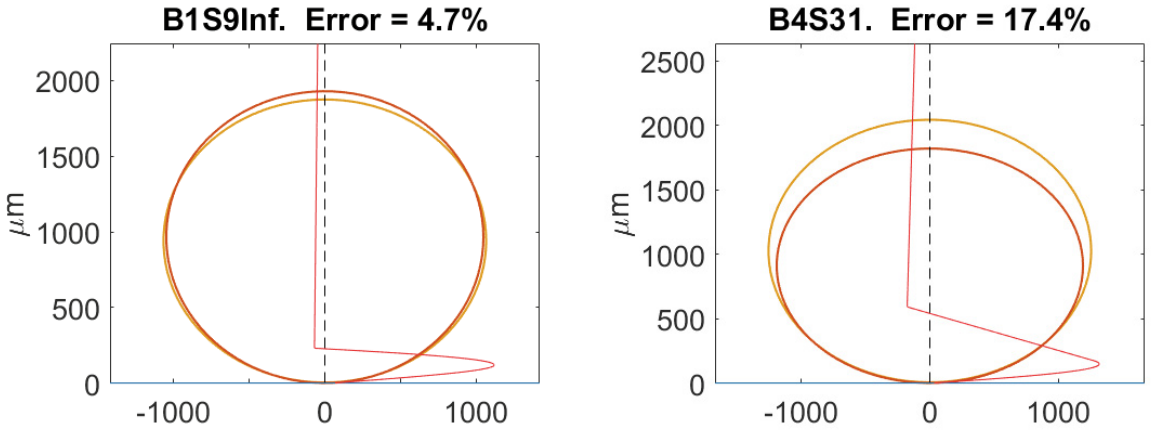

Fig. 6. Elliptical crack shape in the embedded to surface transition situation (yellow) compared with the experimentally observed fractured surface bright region (orange). A sketch of the residual stress profile is added (red) to provide intuition for the length scale. These two examples are representative of the results obtained for all 8 simulations taken into consideration.

6. Conclusions

A systematic procedure to complete a fatigue crack growth simulation is described in a test with a stress gradient due to external load and residual stress distribution and a titanium alloy obtained from additive manufacturing. For a given internal defect, provided its location within the specimen and its geometry are known, fatigue resistance is successfully estimated.

Specimens' fracture surface was investigated and correlated with different crack states. Particularly, an elliptical bright region was observed, even with the naked eye, in a position tangent to the free surface. The shape of this region was correlated to the embedded crack shape at the very moment when embedded to superficial crack transition took place.

Superficial cracks rapidly lead to final failure of the specimen, so embedded to superficial crack transition usually means catastrophic failure in very few cycles.

7. Bibliography

[1] Sanaei, N., Fatemi, A., Phan, N., 2019. Defect characteristics and analysis of their variability in metal L-PBF additive manufacturing. Materials & Design 182, 108091.
[2] Yates, J.R., Efthymiadis, P., Antonysamy, A.A., Pinna, C., Tong, J., 2019. Do additive manufactured parts deserve better? Fatigue & Fracture of Engineering Materials & Structures 42, 2146–2154.
[3] Sterling, A.J., Torries, B., Shamsaei, N., Thompson, S.M., Seely, D.W., 2016. Fatigue behavior and failure mechanisms of direct laser deposited Ti–6Al–4V. Materials Science and Engineering: A 655, 100–112.
[4] Wang, Y., Zhang, S.q., Tian, X.j., Wang, H.m., 2013. High-cycle fatigue crack initiation and propagation in laser melting deposited tc18 titanium alloy. International Journal of Minerals, Metallurgy, and Materials 20, 665–670.
[5] Solberg, K., Guan, S., Razavi, S.M.J., Welo, T., Chan, K.C., Berto, F., 2019. Fatigue of additively manufactured 316L stainless steel: The influence of porosity and surface roughness. Fatigue & Fracture of Engineering Materials & Structures 42, 2043–2052.
[6] Navarro, C., Vázquez, J., Domínguez, J., 2011. A general model to estimate life in notches and fretting fatigue.

Engineering Fracture Mechanics 78, 1590–1601.
[7] Viera-Viera, C., 2019. Comportamiento a fatiga de piezas de titanio (Ti-6Al-4V) fabricadas mediante *selective laser melting*.
[8] Zhai, Y., Galarraga, H., Lados, D.A., 2016. Microstructure, static properties, and fatigue crack growth mechanisms in Ti-6Al-4V fabricated by additive manufacturing: Lens and ebm. Engineering failure analysis 69, 3–14.
[9] Fatemi, A., Molaei, R., Sharifimehr, S., Phan, N., Shamsaei, N., 2017. Multiaxial fatigue behavior of wrought and additive manufactured Ti-6Al-4V including surface finish effect. International Journal of Fatigue 100, 347–366.
[10] Center, N.J.S., 2004. Fatigue crack growth computer program NASGRO version 4.11-reference manual.
[11] Berger, C., Maschinenbau, F.F., 2009. Fracture mechanics proof of strength for engineering components. VDMA.